

Numerical Observation of Disorder-Induced Anomalous Kinetics in the $A + A \rightarrow \emptyset$ Reaction

Won Jae Chung and Michael W. Deem

*Chemical Engineering Department, University of California, Los Angeles, CA
90095-1592*

Abstract

We address via numerical simulation the two-dimensional bimolecular annihilation reaction $A+A \rightarrow \emptyset$ in the presence of quenched, random impurities. Renormalization group calculations have suggested that this reaction displays anomalous kinetics at long times, $c_A(t) \sim at^{\delta-1}$, for certain types of topological or charged species and impurities. Both the exponent and the prefactor depend on the strength of disorder. The decay exponents determined from our simulations agree well with the values predicted by theory. The observed renormalization of the prefactor also agrees well with the values predicted by theory.

1 Introduction

Surface reactions in two-dimensions show a variety of interesting behavior. Qualitatively, the difference between two and three dimensions is that diffusive mixing is less effective in two (and one) dimensions. With less mixing, transport limitations become more significant, and this leads to a breakdown of the law of mass action in two dimensions. Formally, two-dimensions is the upper critical dimension for bimolecular surface reactions [1,2]. The law of mass action, or local chemical kinetics, is the simplest theory with which to predict the reactant concentration in the $A + A \xrightarrow{k} \emptyset$ reaction:

$$\begin{aligned} \frac{dc_A}{dt} &= -kc_A^2 \\ c_A(0) &= n_0 \end{aligned} \tag{1}$$

where k is the reaction rate constant. This theory fails because, without input reactants, the reaction is diffusion limited at long times. The approach of

Eq. (1) does not take into account diffusion limitations, and so this theory cannot be a predictive one. If, in addition, the reaction occurs in a disordered medium, there will be an interplay between the effects of disorder and diffusion limitations, and the simple law of mass action can make no statements about the resulting kinetics. Finally, the law of mass action cannot account for any clustering or other collective behavior of the reactants, since it effectively assumes that the reactants are perfectly well mixed.

A more sophisticated level of theory for chemical reactions is the reaction diffusion partial differential equation:

$$\frac{\partial c_A}{\partial t} = D\nabla^2 c_A + \beta D\nabla \cdot (c_A \nabla v) - kc_A^2 . \quad (2)$$

We will be interested in the case of random initial conditions, where $c_A(\mathbf{x}, 0)$ is a Poisson random number with average n_0 . Here D is the diffusivity, $v(\mathbf{r})$ is the quenched potential in which the reactants diffuse, and $\beta = 1/(k_B T)$ is the inverse temperature. This approach, surprisingly, is also qualitatively wrong in two dimensions. This approach fails because it is a type of mean field theory, and two dimensions is the upper critical dimension for bimolecular kinetics, below which mean field theory fails. If one insists to use Eq. (2), one could predict the true behavior only by using a renormalized, effective reaction rate in place of the bare rate. This effective reaction rate is exactly what the renormalization group treatment of this problem predicts [1,3–5]. What does the reaction diffusion equation leave out, which causes it to miss the renormalization of the effective reaction rate? Technically this approach does not capture the integral occupation number constraint at each site. That is, at each place in space, there can be only an integer number of reactants. This seemingly trivial constraint is what leads to a renormalization of the effective reaction rate.

Previous simulation work has been conducted for a variety of simple reactions in two dimensions. Many simulations have been performed on clean metal surfaces (for a review see [6]). Simple systems, such as oxidation of CO on single crystal Pt(110), show surprisingly rich behavior [7], ranging from spirals and standing waves to chemical turbulence [8,9]. Simulation studies have confirmed several analytical results for the simpler systems (see, for example, [10]). Fascinating effects have been observed on surfaces with patterned disorder [11,12]. Surfaces with spatially random adsorption energies have been shown to lead to a variety of phases observed at steady state [13]. Finally, simulations have been extended to the case of fractal media (see, for example, [14,15]).

Unlike these previous simulation studies, we are interested in the kinetics of the ionic reaction $A^+ + B^- \rightarrow \emptyset$ in two dimensions in the presence of quenched,

charged disorder. The disorder, and the reactants themselves, can either be simple electrostatic charges or topological “charges” such as dislocations or disclinations. For either system, the quenched defects interact with the diffusing reactants via a long-ranged, Coulombic potential energy. The upper critical dimension for this diffusive process is also two. The effects of this disorder are dramatic, and, in fact, the potential energy landscape induced by the random charges is so rugged that the motion is sub-diffusive in two dimensions [16,17]. In other words, this special type of disorder causes the mean square displacement of random walkers to increase sub-linearly with time, $\langle r^2(t) \rangle \sim bt^{1-\delta}$. The scaling exponent is continuously variable in the strength of disorder and can be found exactly [18–24].

Each of the reactions $A + A \rightarrow \emptyset$, $A + B \rightarrow \emptyset$, and $A^+ + B^- \rightleftharpoons AB$ have been studied in the presence of quenched, singular disorder by field-theoretic methods [4,5,25]. Renormalization group theory was used to derive the long-time values for the reactant concentrations. Interestingly, the $A^+ + B^- \rightleftharpoons AB$ ionic reaction at high temperature behaves like the $A + A \rightarrow \emptyset$ model when the back reaction rate is equal to zero [25,26]. This is because the Coulomb interaction between the reactants inhibits the reactant segregation that would otherwise occur in this reaction. We chose to study the $A + A \rightarrow \emptyset$ reaction as a simplified model.

We can understand the results of these renormalization group studies by a simple argument. The $A + A \rightarrow \emptyset$ reaction becomes diffusion limited at long times in the quenched disorder. Simple theory for diffusion-limited reactions, therefore, predicts that the effective rate constant will be proportional to the diffusivity. Since the diffusion is anomalous in this disorder, $\langle r^2(t) \rangle \sim 4Dt(t/t_0)^{-\delta}$, we should expect $k_{\text{eff}} \propto D_{\text{eff}} \sim D(t/t_0)^{-\delta}$, where δ is the same measure of the strength of disorder as above. Here D is the bare diffusivity, and $t_0 = (\Delta r)^2/(2D)$ is a characteristic time for diffusion on a lattice of spacing Δr . We then might expect to use mean field theory with this effective reaction rate to predict the concentration of reactants

$$c_A(t) \sim \frac{1}{k_{\text{eff}}t} \sim \frac{1}{k^*t} \left(\frac{t}{t_0} \right)^\delta \quad \text{as } t \rightarrow \infty, \quad (3)$$

where k^* is some fixed-point effective reaction rate to be determined by a more careful calculation. This simple argument is in agreement with rigorous renormalization group results, which predict [4]

$$k^* = 3\beta^2\gamma D. \quad (4)$$

We here test these renormalization group predictions. We analyze via numerical simulation the behavior of the $A + A \rightarrow \emptyset$ reaction in two-dimensions in

the presence of singular disorder. We calculate by simulation the concentration profiles at long times for various strengths of disorder. We compare both the exponent and the prefactor predicted by renormalization group arguments against those measured via simulation [4]. This paper is organized as follows. In Section 2 we describe the disorder that is appropriate for ionic systems. We express the effects of the quenched disorder in terms of a random potential. In Section 3, we describe the master equation that defines our model of the reaction. We describe a method for numerically solving the master equation by a Poisson process that is effective for strong disorder. In Section 4, we take an alternative approach and describe an exact stochastic partial differential equation (SPDE) that can be derived by field-theoretic means from the master equation. We describe a method for solving the SPDE numerically that is effective for weak disorder. In Section 5, we implement these solution techniques and analyze the long-time behavior of the reactant concentration at various strengths of disorder. We discuss our numerical results in light of the theoretical predictions in Section 6. We conclude in Section 7.

2 The Disorder

The two-dimensional ionic reaction $A^+ + B^- \rightarrow \emptyset$ behaves like the nonionic bimolecular annihilation reaction $A + A \rightarrow \emptyset$ because the Coulomb interaction inhibits the reactant segregation that naturally occurs in the $A + B \rightarrow \emptyset$ reaction [25,26]. This, then, implies that the reactant concentration for the $A^+ + B^- \rightarrow \emptyset$ model is proportional to that for the $A + A \rightarrow \emptyset$ model at long times. The presence of additional, quenched, charged disorder does not change this argument. The $A + A \rightarrow \emptyset$ reaction is much easier to simulate than the ionic $A^+ + B^- \rightarrow \emptyset$ reaction, since one does not have to track the long-range forces between the reactants. For this reason, we choose to simulate the $A + A \rightarrow \emptyset$ model as a general test of the renormalization group predictions for two-dimensional bimolecular reactions in the presence of singular disorder [4,5,25].

The type of physical systems that we have in mind are systems with “ionic” disorders. Such disorder could occur, for example, on the surface of an ionic crystalline lattice. Imagine that the lattice has line defects caused by dislocation line pairs forming line vacancies or line interstitials. If these defects were immobile, they would generate a random, quenched electrostatic potential on the surface. The interaction between ionic reactants on the surface and these line charges would be logarithmic, which is technically “relevant” in two dimensions. The $1/r$ interactions between the ions themselves is technically “irrelevant” and can be ignored.

Alternatively, our system can be viewed as modeling the dynamics of a collec-

tion of line dislocations in a solid. The hexatic-solid transition in two dimensional monolayers occurs by pairing of dislocations and is a good example of an ionic reaction, albeit with vector “charges” [27]. If there were some additional dislocations pinned by defects, these defects would interact logarithmically with the moving dislocations, just as in our model. A physical system that more closely resembles our model is the liquid-hexatic transition in two dimensional fluids. Here the transition occurs by pairing of disclinations, which are a perfect manifestation of topological charges that interact logarithmically [27]. Additional, pinned disclinations would generate the quenched disorder present in our model.

Experiments have, indeed, seen effects of pinned disorder on the liquid-hexatic transition for both flux lines in charged density wave systems [28,29] and surfactants in hexatic multilayers in Langmuir-Blodgett films [30]. Detailed renormalization group calculations are in agreement with the observed effects [25]. An additional physical system, for which experiments could be performed, are charged vortices in a thin fluid film between two spatially-addressable electrodes [31].

We use a quenched random potential to represent the potential induced by the immobile defects. The random potential is Gaussian at long wavelengths [32], and the appropriate form of the potential-potential correlation function at long wavelengths is

$$\hat{\chi}_{vv}(k) \sim \gamma/k^2 . \quad (5)$$

Here γ is a measure of the strength of disorder. It is roughly proportional to the square of the density of defects. Our simulation takes place on a square lattice, and a natural form of the potential-potential correlation function is

$$\hat{\chi}_{vv}(k_x, k_y) = \frac{\gamma(\Delta r)^2}{4 - 2 \cos(k_x \Delta r) - 2 \cos(k_y \Delta r)} , \quad (6)$$

where Δr is the lattice spacing. This form reduces to that of Eq. (5) at long wavelengths, $k \rightarrow 0$, and in the limit of small lattice spacing, $\Delta r \rightarrow 0$. We generate the random potential $v(\mathbf{r})$ by first generating $\hat{v}(\mathbf{k})$ in Fourier space, where the values at different wave vectors are independent Gaussian random numbers, and then performing an inverse fast Fourier transform [33,34]. We use periodic boundary conditions for the random lattice.

A random potential of this form is known to have a significant effect on diffusing species, resulting in an anomalous mean square displacement at long

times [16–24]

$$\langle r^2(t) \rangle \sim 4Dt \left(\frac{t}{t_0} \right)^{-\delta} . \quad (7)$$

The scaling exponent, $1 - \delta$, depends on the strength of disorder. For Gaussian disorder, the exponent is exactly given by

$$\delta = \left[1 + \frac{8\pi}{\beta^2 \gamma} \right]^{-1} . \quad (8)$$

3 The $A + A \rightarrow \emptyset$ Reaction

Our model of the $A + A \rightarrow \emptyset$ reaction can be defined mathematically by a master equation. We assume that the reaction takes place on a square $N \times N$ lattice with lattice spacing Δr . The reactants move diffusively in a random potential on the lattice. The reactants annihilate at rate k whenever two meet on the same lattice site. The master equation describes how the probability of each possible configuration of particles on the lattice, $P(\{n_i\}, t)$, changes with time. The appropriate master equation for our system is

$$\begin{aligned} \frac{\partial P(\{n_i\}, t)}{\partial t} = & \sum_{ij} [\tau_{ji}^{-1} (n_j + 1) P(\dots, n_i - 1, n_j + 1, \dots, t) - \tau_{ij}^{-1} n_i P] \\ & + \frac{k}{2(\Delta r)^2} \sum_i [(n_i + 2)(n_i + 1) P(\dots, n_i + 2, \dots, t) \\ & - n_i(n_i - 1) P] \end{aligned} \quad (9)$$

where n_i is the number of particles at site i , D is the diffusivity, k is the reaction rate constant, and Δr is the lattice spacing. Here τ_{ij}^{-1} , to be defined below, is the rate at which particles hop from lattice site i to nearest neighbor lattice site j . The summation over i is over all sites on the lattice and the summation over j is over all nearest neighbors of site i . We place the reactants randomly on the lattice at time $t = 0$. The initial concentration at any given site will, thus, be Poisson, with average density that we define to be n_0 :

$$\begin{aligned} P(n_i) &= \frac{[n_0(\Delta r)^2]^{n_i}}{n_i!} e^{-n_0(\Delta r)^2} \\ \langle n_i / (\Delta r)^2 \rangle &= n_0 , \end{aligned} \quad (10)$$

This master equation can be solved exactly by directly considering the particle

reaction and diffusion process [35]. The master equation implies that a given configuration of reactants on the lattice follows a continuous-time, Markovian, Poisson process. In this process, all possible changes to the lattice configuration occur at specific rates. That is, both the reaction and diffusion moves have rates. The rates of diffusion depend on the values of the potential on the lattice. Certain moves are favored over others, due to local gradients in the potential. The rate of hopping to a nearest neighbor site is τ_{ij}^{-1} . There are four of these rates at each lattice site. The rate for hopping to the right is

$$\tau_{\text{R}}^{-1}(x, y) = \frac{D}{(\Delta r)^2} \exp \{ \beta [v(x, y) - v(x + \Delta r, y)] / 2 \} , \quad (11)$$

for hopping to the left is

$$\tau_{\text{L}}^{-1}(x, y) = \frac{D}{(\Delta r)^2} \exp \{ \beta [v(x, y) - v(x - \Delta r, y)] / 2 \} , \quad (12)$$

for hopping above is

$$\tau_{\text{U}}^{-1}(x, y) = \frac{D}{(\Delta r)^2} \exp \{ \beta [v(x, y) - v(x, y + \Delta r)] / 2 \} , \quad (13)$$

and for hopping below is

$$\tau_{\text{D}}^{-1}(x, y) = \frac{D}{(\Delta r)^2} \exp \{ \beta [v(x, y) - v(x, y - \Delta r)] / 2 \} . \quad (14)$$

At each lattice site, there are $n_i(n_i - 1)/2$ possible reaction moves. Each of these moves has the rate

$$\tau_{\text{rxn}}^{-1} = \frac{k}{(\Delta r)^2} . \quad (15)$$

Overall, for the whole lattice there are $4 \sum_i n_i$ possible diffusion moves and $\sum_i n_i(n_i - 1)/2$ possible reaction moves.

A Markov process is initiated by placing the particles randomly on the surface, with average density n_0 . The Markov chain is then generated by picking one of these possible events according to its probability of occurrence and incrementing time according to its rate of occurrence. The probability of event α occurring, out of all the possible diffusion and reaction moves, is

$$P(\text{event } \alpha) = \frac{\tau_{\alpha}^{-1}}{\sum_{\gamma} \tau_{\gamma}^{-1}} . \quad (16)$$

Since the process is Poisson, time is incremented by

$$\Delta t = \frac{-\log \zeta}{\sum_{\gamma} \tau_{\gamma}^{-1}}, \quad (17)$$

where ζ is a uniformly distributed random number between zero and one. This step of the Markov chain is repeated until only zero or one particles remain on the lattice.

We find this procedure to be efficient when the strength of disorder, $\beta^2\gamma$, is large. For computational convenience, we make two approximations. First, when a particle moves to a site that is already occupied by another particle, the annihilation reaction occurs immediately. In other words, we set the reaction rate, k , equal to infinity. Note that the renormalization group predictions are independent of the bare reaction rate [4]. Physically this is because the reaction is diffusion-limited at long times, and so the bare reaction rate does not matter. Second, we assume that each particle has an equal probability of being moved

$$P(\text{moving particle } \alpha) = \frac{1}{n}, \quad (18)$$

where n is the total number of particles on the lattice. The direction of movement of a chosen particle, however, is specified by the local gradient of the random potential, as in Eqs. (11-14). Specifically, we generate another uniformly distributed random number, which is compared against the four different hop probabilities:

$$P(\text{hop } i) = \frac{\tau_i^{-1}}{\sum_j \tau_j^{-1}}. \quad (19)$$

The chosen move is performed, and time is incremented by $\Delta t = N^2 / (n \sum_{ij} \tau_{ij}^{-1})$. The uniform choice of reactant to move and the approximate time incrementation are both exact in the long-time limit when $\Delta r \rightarrow 0$ in the hopping rates (11)-(14).

4 The Stochastic Equation

Alternately, we can derive a stochastic partial differential equation by mapping the master equation onto a field theory. The field theory looks like a Bosonic quantum field theory due to the constraint of an integral occupation number at

each lattice site. The continuous-time stochastic partial differential equation for the $A + A \rightarrow \emptyset$ reaction is [4]

$$\begin{aligned} \frac{\partial a}{\partial t} &= D\nabla^2 a + \beta D\nabla \cdot (a\nabla v) - ka^2 + i\eta a \\ a(\mathbf{x}, 0) &= n_0, \end{aligned} \tag{20}$$

where the real, Gaussian random field $\eta(\mathbf{x}, t)$ has zero mean and variance $\langle \eta(\mathbf{x}, t)\eta(\mathbf{x}', t') \rangle = k\delta(\mathbf{x} - \mathbf{x}')\delta(t - t')$. The physical concentration is given by taking the average of the solution over the random field η . Since the reaction occurs on a lattice, the spatial derivative symbols are actually a shorthand for finite difference expressions. The field-theoretic derivation shows that this stochastic differential equation should be interpreted in the Itô sense.

The stochastic partial differential equation was solved numerically by using a second-order, semi-implicit method. This method gives exact solutions to the master equation without any approximations, in the limit that the integration time step tends to zero. The process of solving the stochastic partial differential equation takes place on a square lattice. We define $b[a(x, y, t)] = D\nabla^2 a - ka^2$ and $\mu = \sqrt{k}/\Delta r$. An explicit method for Eq. (20) equation is given by [36]

$$\begin{aligned} a(x, y, t + \Delta t) &= a(x, y, t) \\ &+ \frac{\Delta t}{2} \left\{ b[a(x, y, t)] + b \left[a(x, y, t) + i\mu\sqrt{t}a(x, y, t)z(x, y, t) \right. \right. \\ &\quad \left. \left. + \Delta t b[a(x, y, t)] \right] \right\} \\ &+ i\mu\sqrt{t} \left[a(x, y, t) + \frac{\Delta t}{2} b[a(x, y, t)] \right] z(x, y, t) \\ &- \frac{\Delta t}{2} \mu^2 a(x, y, t) [z(x, y, t)^2 - 1]. \end{aligned} \tag{21}$$

Here $z(x, y, t)$ is a Gaussian random number of unit variance. These random numbers are uncorrelated at different positions and times. This numerical method is accurate to $O[(\Delta t)^2]$ in the weak sense. A semi-implicit method is generated by replacing $b[a + i\mu\sqrt{t}az + \Delta t b(a)]$ on the right hand side with $b[a(x, y, t + \Delta t)]$. This semi-implicit method is also accurate to $O[(\Delta t)^2]$ in the weak sense. Direct implementation of this approach leads to a complicated, non-linear matrix equation to solve. We use, instead, an operator-splitting approach [37]. On even integration time steps, we use a method implicit in the x -diffusion terms and explicit in the y -diffusion and reaction terms. On odd integration time steps, we use a method implicit in the y -diffusion terms and explicit in the x -diffusion and reaction terms. This operator-splitting, semi-implicit approach leads to tridiagonal matrix equations that are simple to solve. We found that including a time step implicit in the reaction terms was

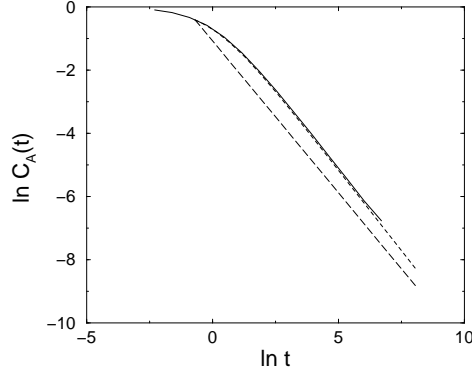


Fig. 1. The reactant concentration as a function of time for $\beta^2\gamma = 1$, $k = 1$, and $n_0 = 1$. The simulation data are shown by the solid line. The long-time value predicted by renormalization group arguments is shown by the long-dashed line. The concentration predicted by renormalization group calculations for all times is shown by the short-dashed line. At times longer than those shown here, the two dashed lines converge.

not useful. The periodic boundary conditions enter these equations through the finite-difference definition of the diffusion terms.

5 Results

For weak disorder, $\beta^2\gamma < 1$, the master equation was solved by numerically integrating the exact stochastic differential equation. The concentrations produced in a typical simulation run are illustrated in Figure 1. The simulation values at short times are quite far off from the long-time values predicted by the renormalization group treatment. This is because the asymptotic scaling of the reaction concentration is reached only for very long times for the parameters of Figure 1. At very long times, for a sufficiently large lattice, the concentration observed by simulation would be the asymptotic value predicted by theory. To achieve an agreement between theory and simulation, we also show in Figure 1 the concentration predicted for all times with the use of the running coupling in Eq. (1). This approximate concentration profile is derived in a straight-forward fashion from the flow equations for this system [4]:

$$c(t) = \frac{(t/t_0)^{\delta-1}}{n_0(t/t_0)^{\delta-1} + k(l^*)t_0}$$

$$k(l^*) = \frac{3\beta^2\gamma D}{1 + (3\beta^2\gamma D/k_0 - 1)(t/t_0)^{-3\delta}} . \quad (22)$$

As we can see from this more detailed theoretical prediction, the renormalization of the effective reaction rate to the asymptotic value is rather slow,

occurring as $(t/t_0)^{-3\delta}$. At long times, the level of noise in the simulation data becomes more significant. This is because there are fewer particles at longer times, and so the statistical error is greater. If a greater lattice size or a smaller time step were used, then less noise would be observed at these times. Balancing these considerations against computational feasibility, we chose to use 2048×2048 square lattices.

The slow renormalization of the effective reaction rate prevents a direct simulation of the reaction for arbitrary values of the parameters. To counteract the effect of the slow renormalization, we performed additional simulations by starting with the renormalized reaction rate predicted from theory, $k = k^* = 3\beta^2\gamma D$. For runs with this initial value of the reaction rate, the concentrations reach the asymptotic scaling at fairly short times.

To determine the observed values of the the decay exponent, $1 - \delta^*$, and the renormalized reaction rate, k^* , a log-log plot is made for the concentration of species A versus time. The slope of this plot gives us the renormalized decay exponent, and the y-intercept gives us the renormalized reaction rate. With this method, far more data points will be plotted and used at long times than intermediate times in the fit to determine the renormalized values. Therefore, the values determined from the fit will be heavily biased by data points gathered at long times. This biasing is artificial, since the concentration profile must be continuous as a function of time, and so we should not overweight the long-time section. To eliminate this bias, we used data points in powers of two to perform the fits. For example, data points corresponding to times steps 1, 2, 4, 8, 16, 32, 64, ... were used to determine the slope and the prefactor. Note that to determine k^* we need to assume a value for t_0 . We use $t_0 = (\Delta r)^2/(2D)$, which is suggested by simple perturbation theory for this problem.

Figure 2 compares the exponent of the concentration decay observed by simulation with that predicted by theory. Figure 3 compares the effective reaction rate observed by simulation with that predicted by theory. These two plots show that the theoretical values agree well with those obtained by simulation. The error bars were determined by considering both random and systematic errors. We found that the most conservative method was to vary the smallest time at which we start the fit. We found that the slope and prefactor were somewhat sensitive to which data points were used in the calculations. The error bars encompass both the random, statistical errors and the systematic error associated with the range of data that we fit.

For strong disorder, $\beta^2\gamma > 1$, the approximate Poisson process was used to solve the master equation. For each set of parameters, we performed 10 simulations on 2048×2048 lattices to generate average concentration profiles. As before, a $\log c_A$ versus $\log t$ plot of the simulation data was used to determine

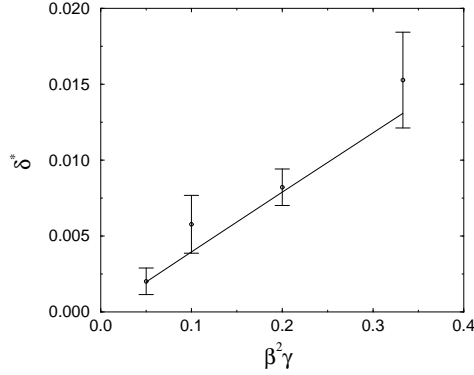


Fig. 2. Presented are the observed values for the exponent of the reaction concentration decay, determined from $c_A(t) \sim at^{\delta^*-1}$, as a function of the strength of disorder. Renormalization group predictions are shown by the solid line.

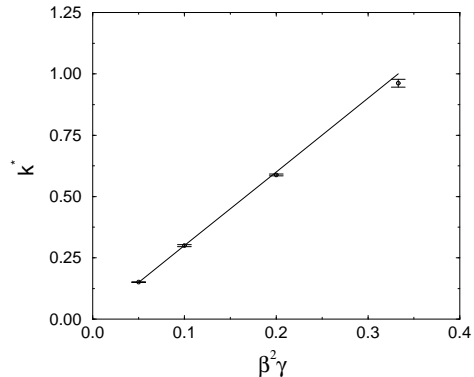


Fig. 3. Presented are the observed values of the renormalized reaction rate, determined from $c_A(t) \sim (t/t_0)^{\delta^*}/(k^*t)$, as a function of the strength of disorder. Renormalization group predictions are shown by the solid line.

the decay exponent, $1 - \delta^*$, and the renormalized reaction rate, k^* . Also as before, we used data exponentially spaced in time. For strong disorder, the renormalization of the effective reaction rate constant occurs very quickly.

Figure 4 compares the exponent of the concentration decay observed by simulation with that predicted by theory. Figure 5 compares the effective reaction rate observed by simulation with that predicted by theory.

6 Discussion

The most significant prediction of the renormalization group studies is the decay exponent, $c_A(t) \sim at^{1-\delta}$, where δ is given by Eq. (8). All simulations for weak disorder, $\beta^2\gamma < 1$, show an observed slope that is in agreement with this prediction, to within the error bars. This is significant, since the renormalization group studies are, in principle, expansions in the parameter

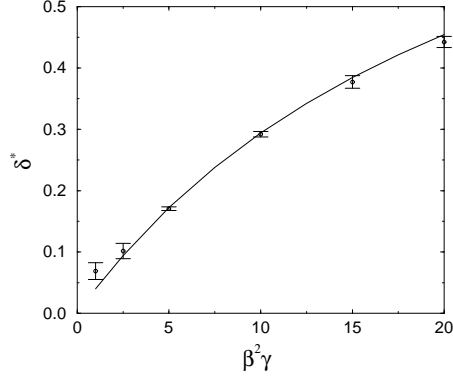


Fig. 4. Presented are the observed values for the exponent of the reaction concentration decay, determined from $c_A(t) \sim at^{\delta^*-1}$, as a function of the strength of disorder. Renormalization group predictions are shown by the solid line.

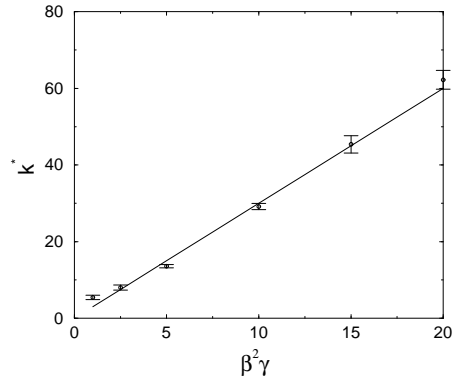


Fig. 5. Presented are the observed values of the renormalized reaction rate, determined from $c_A(t) \sim (t/t_0)^{\delta^*}/(k^*t)$, as a function of the strength of disorder. Renormalization group predictions are shown by the solid line.

$\beta^2\gamma$, and so the predictions are strictly accurate only for weak disorder. It was anticipated in the renormalization group treatment, however, that the result for the decay exponent may be exact to all orders of $\beta^2\gamma$ [4].

For strong disorder, $\beta^2\gamma > 1$, some small discrepancies exist between the simulation and the theoretical predictions for the decay exponent. The approximate Poisson process method that we used to solve the master equation requires the effective reaction rate to renormalize from infinity to k^* . This process occurs slowly for weak disorder, as shown by Eq. (22), and this is the reason for the discrepancy for $\beta^2\gamma \approx 1$. Simulations on lattices larger than 2048×2048 , which would provide data to lower concentrations, would eventually yield an exponent in agreement with the predicted value.

The renormalization group studies also predict the fixed-point value of the effective reaction rate, Eq. (4). This prediction, strictly speaking, is an expansion in the disorder strength, and we would generally expect there to be corrections higher order in $\beta^2\gamma$. All of the simulations for weak disorder are

in agreement with this prediction. For $\beta^2\gamma \approx 0.33$, there is a small discrepancy not contained within the error bars. The numerical integration of Eq. (20) is exceedingly difficult for large $\beta^2\gamma$, and the small discrepancy between simulation and theory is most likely due to use of a time step that was not quite small enough. Resolution of this discrepancy would have required an integration time step substantially smaller than is feasible, even on our high-performance workstations.

Even for strong disorder, the simulations show an effective reaction rate in agreement with the predicted values. This is significant on two counts. First, the renormalization group predictions are only a first order approximation for k^* , and it is surprising that the higher order corrections are so small for $\beta^2\gamma \approx 20$. Second, the simulation technique for strong disorder requires the effective reaction rate to renormalize from infinity to a finite k^* . That this happens so effectively is impressive. The discrepancies in the observed effective reaction rate for $\beta^2\gamma \approx 1$ are, again, due to the slow renormalization of the effective reaction rate.

7 Conclusions

Our numerical simulation of the $A + A \xrightarrow{k} \emptyset$ reaction is in agreement with the field-theoretic renormalization group predictions [4]. An anomalous decay exponent, predicted by the renormalization group studies, is observed. No significant discrepancy between the numerical and analytical predictions are observed over a wide range of disorder strengths. More impressively, the effective reaction rate observed from the numerical simulations is in quantitative agreement with the renormalization group predictions for the same wide range of disorder strengths. This agreement is unexpected and may signify that the one-loop renormalization group results are more accurate than anticipated. With these simulations, we now have satisfying agreement between rigorous field-theoretic results, simple physical arguments, and exact numerical results for this interesting case of anomalous kinetics.

Acknowledgments

This research was supported by the National Science Foundation through grants CHE-9705165 and CTS-9702403.

References

- [1] L. Peliti, J. Phys. A **19**, L365 (1986).
- [2] B. P. Lee and J. Cardy, J. Stat. Phys. **80**, 971 (1995); **87**, 951 (1997).
- [3] B. P. Lee, J. Phys. A **27**, 2633 (1994).
- [4] J.-M. Park and M. W. Deem, Phys. Rev. E **57**, 3618 (1998).
- [5] M. W. Deem and J.-M. Park, Phys. Rev. E **57**, 2681 (1998).
- [6] H. C. Kang and W. H. Weinberg, Chem. Rev. **95**, 667 (1995).
- [7] M. D. Graham *et al.*, Science **264**, 80 (1994).
- [8] M. Eiswirth and G. Ertl, in *Chemical Waves and Patterns*, edited by R. Kapral and K. Showalter (Kluwer, Dordrecht, 1995).
- [9] S. Jakubith *et al.*, Phys. Rev. Lett. **65**, 3013 (1990).
- [10] P. Argyrakis, R. Kopelman, and K. Lindenberg, Chem. Phys. **177**, 693 (1993).
- [11] M. Bar *et al.*, J. Chem. Phys. **100**, 19106 (1996).
- [12] N. Hartmann *et al.*, Phys. Rev. Lett. **76**, 1384 (1996).
- [13] L. Frachebourg, P. L. Krapivsky, and S. Redner, Phys. Rev. Lett. **75**, 2891 (1995).
- [14] G. Zumofen, J. Klafter, and A. Blumen, J. Stat. Phys. **65**, 1015 (1991).
- [15] R. Kopelman, Science **241**, 1620 (1988).
- [16] D. S. Fisher *et al.*, Phys. Rev. A **31**, 3841 (1985).
- [17] V. E. Kravtsov, I. V. Lerner, and V. I. Yudson, J. Phys. A **18**, L703 (1985).
- [18] V. E. Kravtsov, I. V. Lerner, and V. I. Yudson, Phys. Lett. A **119**, 203 (1986).
- [19] J. P. Bouchaud, A. Comtet, A. Georges, and P. L. Doussal, J. Phys **48**, 1445 (1987).
- [20] J. P. Bouchaud, A. Comtet, A. Georges, and P. L. Doussal, J. Phys **49**, 369 (1988).
- [21] J. Honkonen, Y. M. Pis'mak, and A. V. Vasil'ev, J. Phys. A **21**, L835 (1988).
- [22] J. Honkonen and Y. M. Pis'mak, J. Phys. A **22**, L899 (1989).
- [23] S. É. Derkachov, J. Honkonen, and Y. M. Pis'mak, J. Phys. A **23**, L735 (1990).
- [24] S. É. Derkachov, J. Honkonen, and Y. M. Pis'mak, J. Phys. A **23**, 5563 (1990).
- [25] J.-M. Park and M. W. Deem, Phys. Rev. E **58**, 1487 (1998).

- [26] D. Toussaint and F. Wilczek, *J. Chem. Phys.* **78**, 2642 (1983).
- [27] D. R. Nelson, in *Phase Transitions and Critical Phenomena*, edited by C. Domb and J. Lebowitz (Academic Press, New York, 1983), Vol. 7.
- [28] H. J. Dai and C. M. Lieber, *Phys. Rev. Lett.* **69**, 1576 (1992).
- [29] H. J. Dai, J. Liu, and C. M. Lieber, *Phys. Rev. Lett.* **72**, 748 (1994).
- [30] R. Viswanathan, L. L. Madsen, J. A. Zasadzinski, and D. K. Schwartz, *Science* **269**, 51 (1995).
- [31] O. Paireau and P. Tabeling, *Phys. Rev. E* **56**, 2287 (1997).
- [32] M. W. Deem and D. Chandler, *J. Stat. Phys.* **76**, 911 (1994).
- [33] M. W. Deem, *J. Chem. Phys.* **98**, 1002 (1994).
- [34] V. Pham and M. W. Deem, *J. Phys. A* **31**, 7235 (1998).
- [35] T. Elston and C. Doering, *J. Stat. Phys.* **83**, 359 (1996).
- [36] W. P. Petersen, *J. Comput. Phys.* **113**, 75 (1994).
- [37] W. H. Press, B. P. Flannery, S. A. Teukolsky, and W. T. Vetterling, *Numerical Recipes in Fortran*, 2nd ed. (Cambridge University Press, New York, 1992).